# Boosting energy-efficient hydrogen evolution by electronically modulating Ni-nodes in a framework for methanol oxidation in fresh and seawater

Nabeen K. Shrestha,*Akbar I. Inamdar, Hyunsik Im, Sangeun Cho*

Division of System Semiconductor, College of AI Convergence, Dongguk University, Seoul 04620, Republic of Korea.

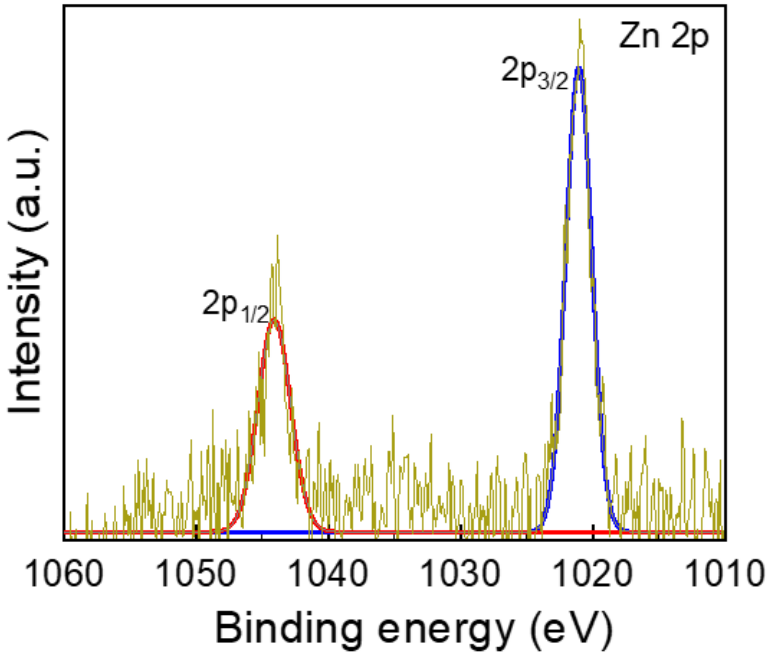


**Figure S1**. XPS core level spectrum of Zn 2p in e-Ni MOF.

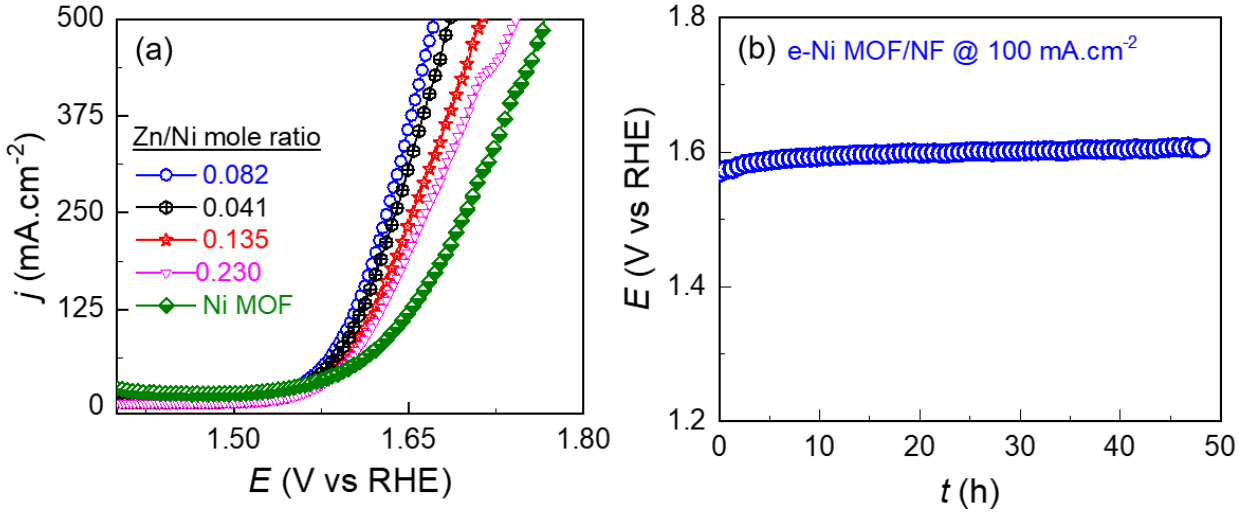


**Figure S2**. (a) LSV curves of various concentration of $Zn^{2+}$ doped Ni MOF films on nickel foam (NF) substrate measured in 1.0 M methanol added 1.0 M KOH solution at a scanning rate of 5 $mVs^{-1}$. (b) Chronopotentiometric stability curve of the e-Ni MOF/NF electrode measured over 48 hours in 1.0 M KOH solution at 100 $mA.cm^{-2}$.

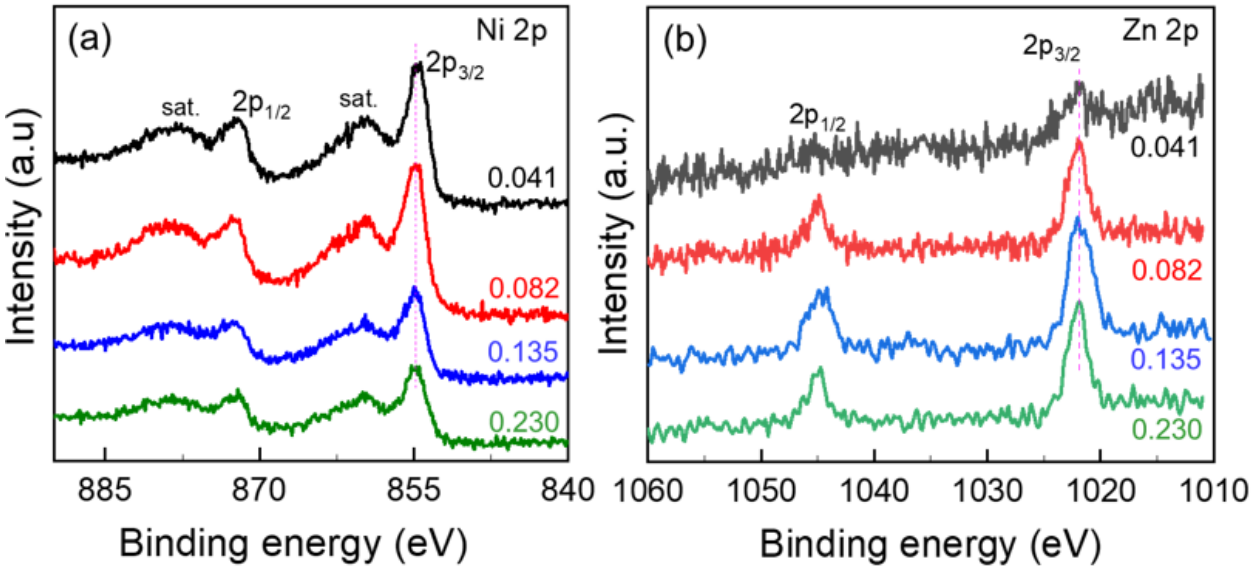


**Figure S3**. XPS spectra of (a) Ni 2p and (b) Zn 2p for the Zn-doped Ni MOFs having Zn/Ni mole ratios of 0.041 to 0.230.

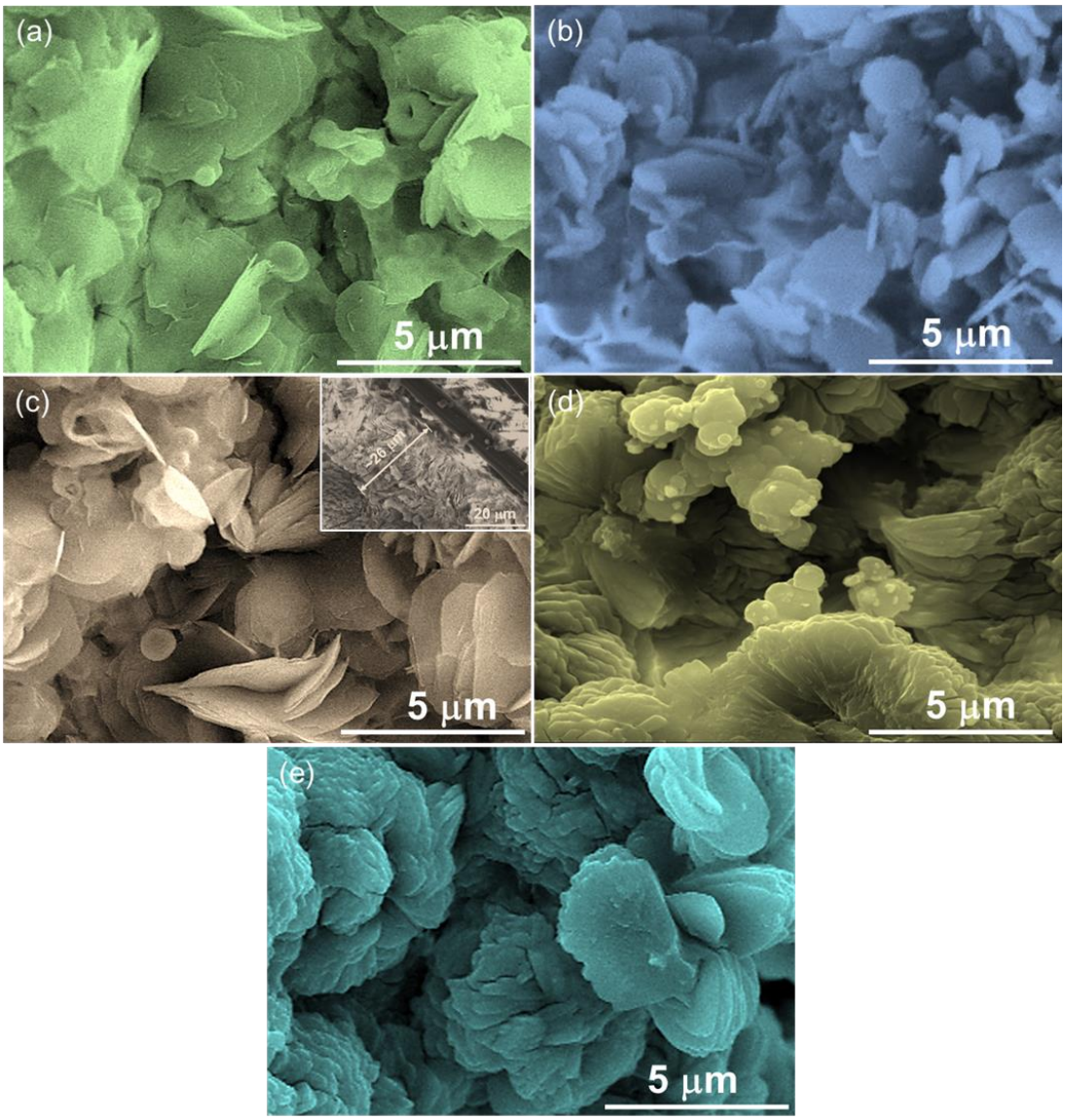


**Figure S4**. SEM images of the (a) pristine Ni MOF, and (b) Zn doped Ni MOFs films on a nickel foam having Zn/Ni mole ratios of (b) 0.041, (c) 0.081, (d) 0.135, and (e) 0.230. The inset image of figure "(c)" is the cross-sectional SEM image representing the MOF film thickness, which was obtained by depositing the MOF film on a carbon-fiber paper under the same conditions that were employed to deposit the film on a nickel foam substrate.

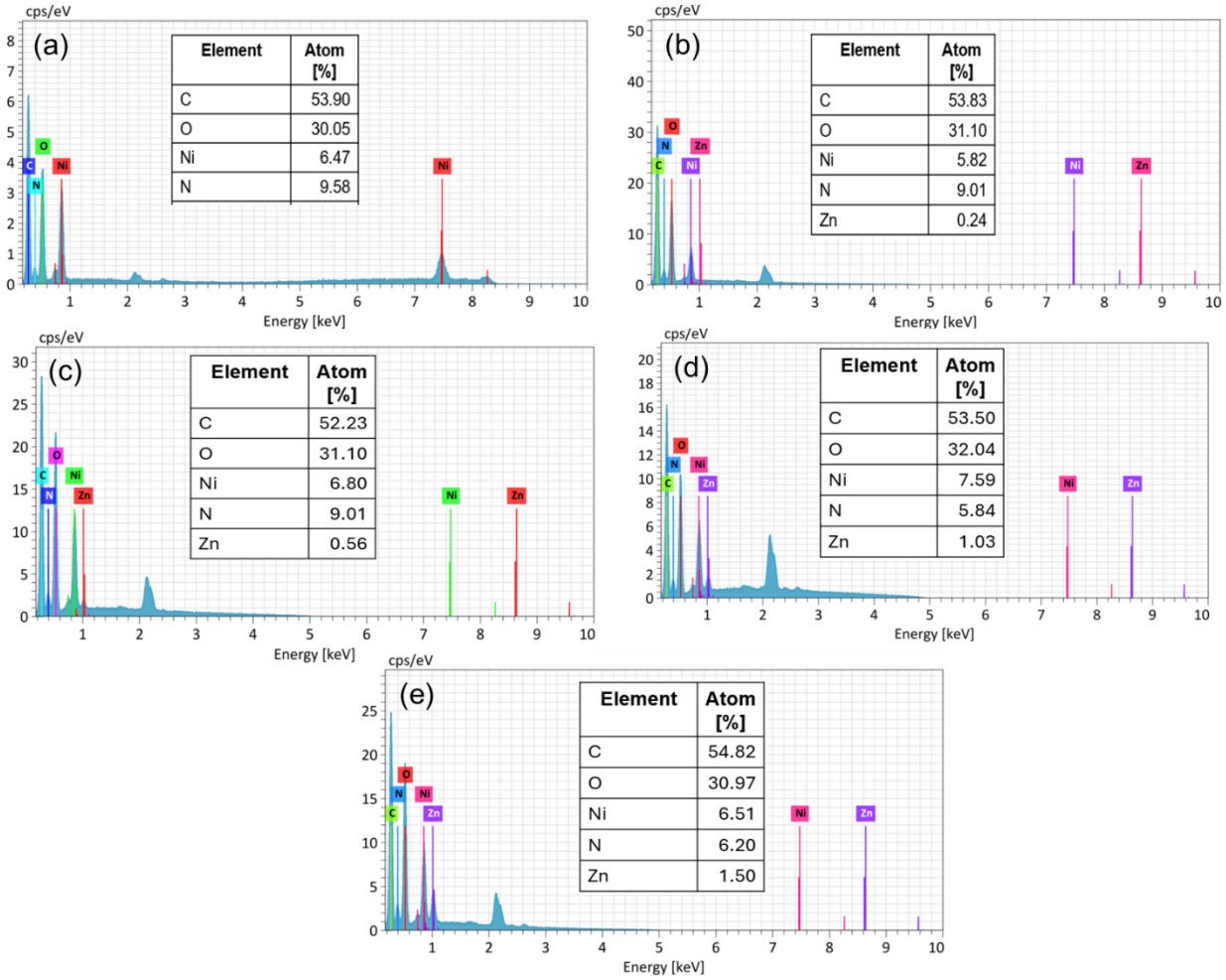


**Figure S5**. EDX spectra and the corresponding element composition of the (a) pristine Ni MOF, and Zn-doped Ni MOF showing Zn/Ni mole ratios of (b) 0.041, (c) 0.081, (d) 0.135, and (e) 0.230.

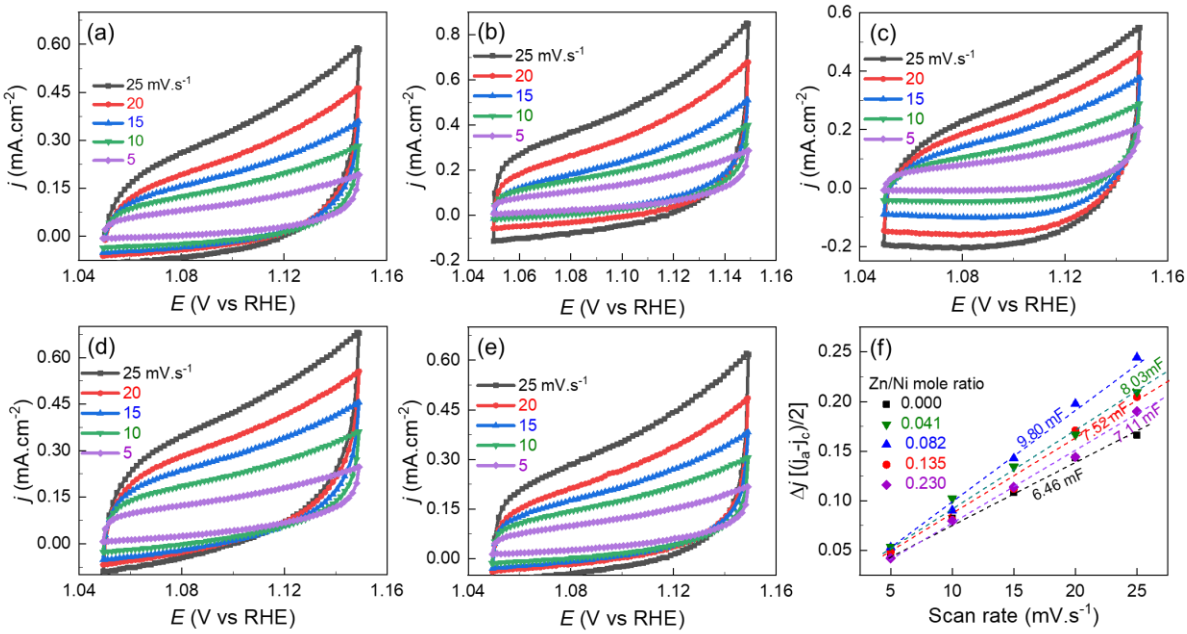


**Figure S6**. Cyclic voltammograms of the MOF films on NF substrate measured at various scan rates in a non-Faradic potential window in 1.0 M KOH solution (a) pristine Ni MOF, and Zn-doped Ni MOFs having Zn/Ni mole ratios of (b) 0.041, (c) 0.082, (d) 0.135, (e) 0.230. (f) Average current density at 1.10 V vs RHE as a function of scan rate plots executed from the corresponding cyclic voltammograms. The slopes of the straight lines provide the double layer capacitance ($C_{dl}$).

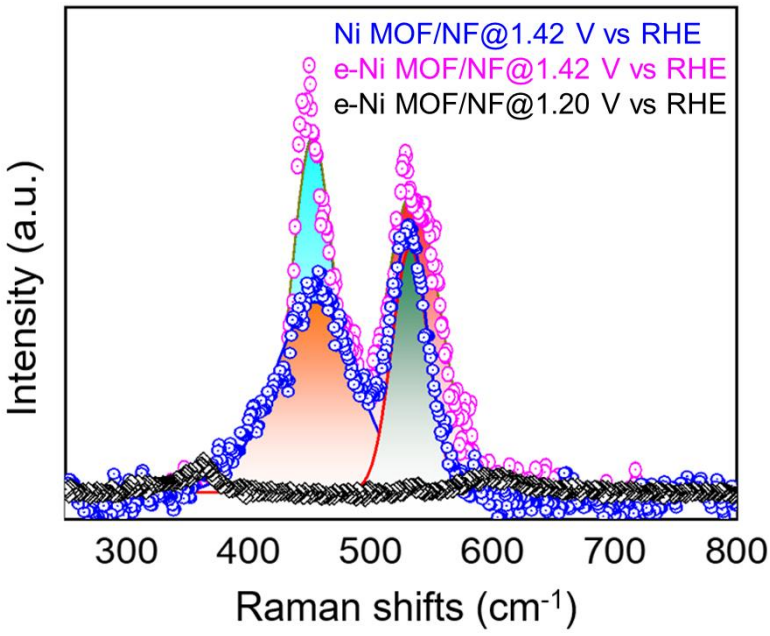


**Figure S7**. Raman spectra of the MOF/NF electrode measured after polarization for 5 minutes in 1.0 M methanol added 1.0 M KOH solution.

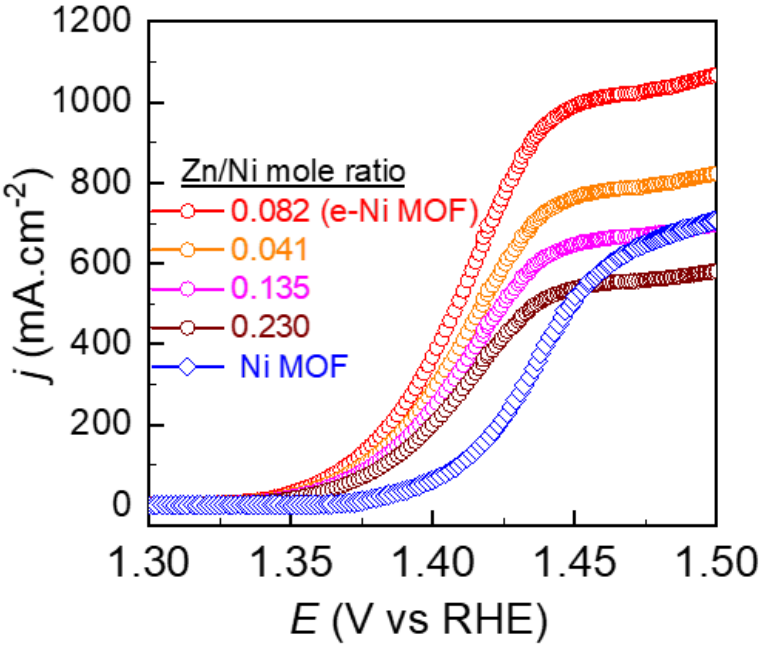


**Figure S8**. LSV curves of the pristine, and various concentration of $Zn^{2+}$ doped Ni MOF films on nickel foam (NF) substrate measured in 1.0 M KOH solution at a scanning rate of 5 $mVs^{-1}$.

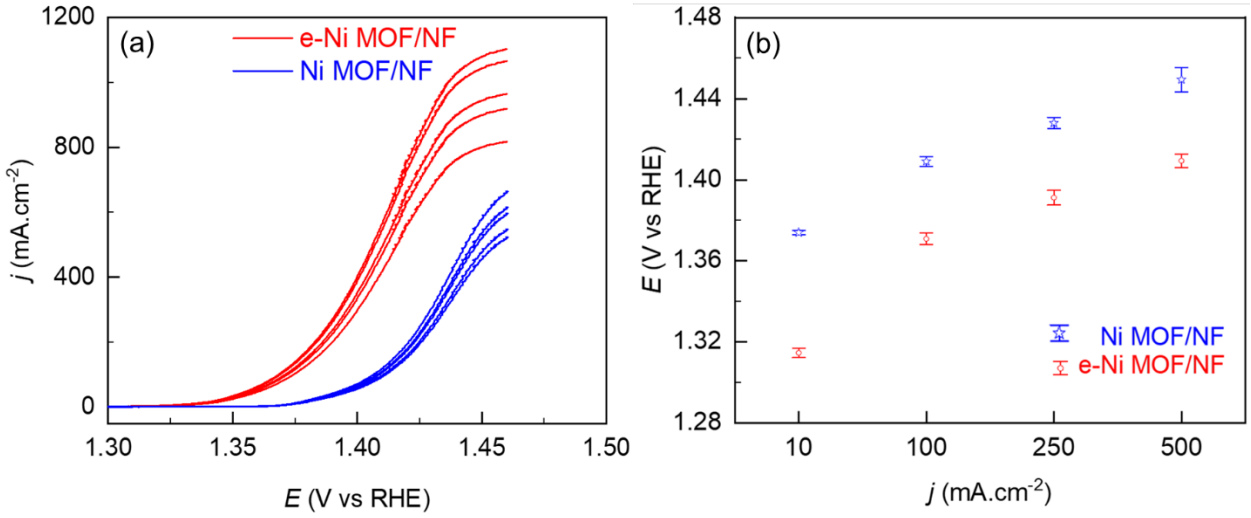


**Figure S9**. (a) LSV curves of 5-replicas of the pristine Ni MOF/NF and e-Ni MOF/NF electrode in 1.0 M methanol added 1.0 M KOH solution at a scanning rate of 5 $mV.s^{-1}$. (b) Cross ponding MeOR oxidation potentials at different electrolysis current densities with error bars.

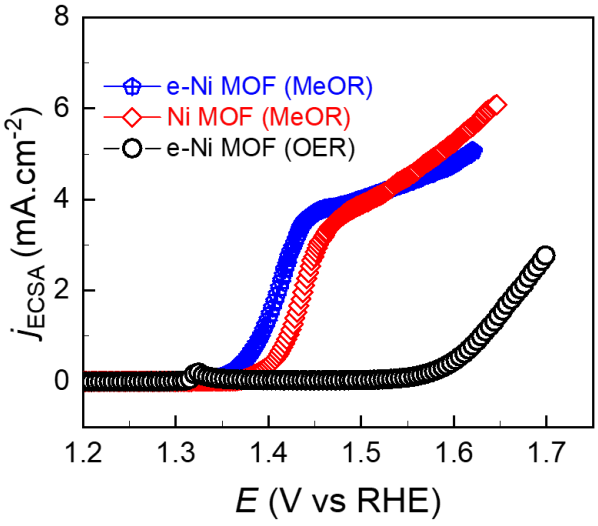


**Figure S10**. ECSA normalized LSV curves of MOF films on NF substrate measured with (MeOR) and without (OER) 1.0 M methanol added 1.0 M KOH solution at a scanning rate of 5 $mVs^{-1}$.

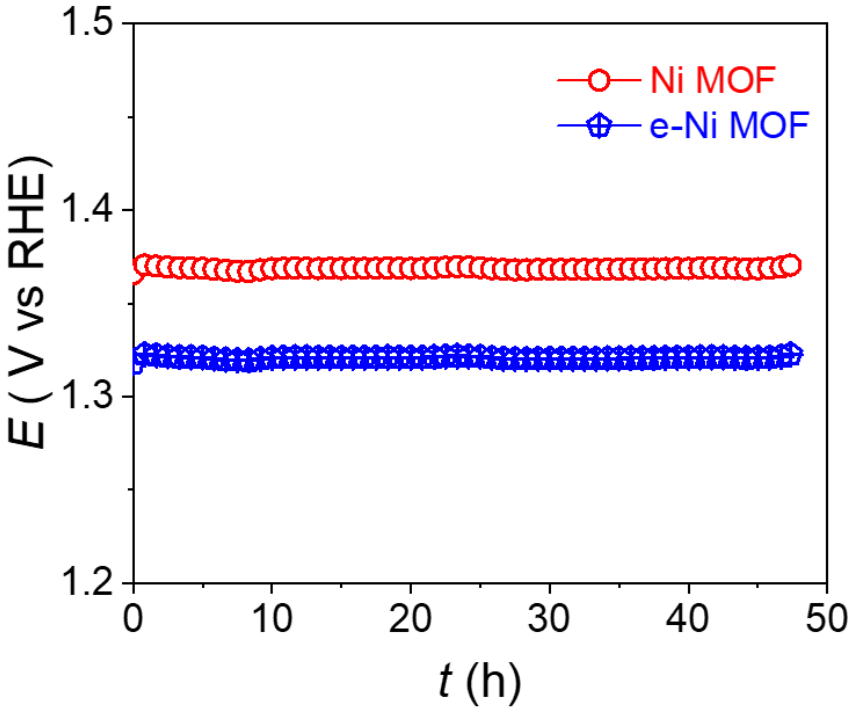


**Figure S11**. Chronopotentiometric stability curves of the MOF/NF electrodes measured over 48 hours in 1.0 M methanol added 1.0 M KOH solution at 10 $mA.cm^{-2}$.

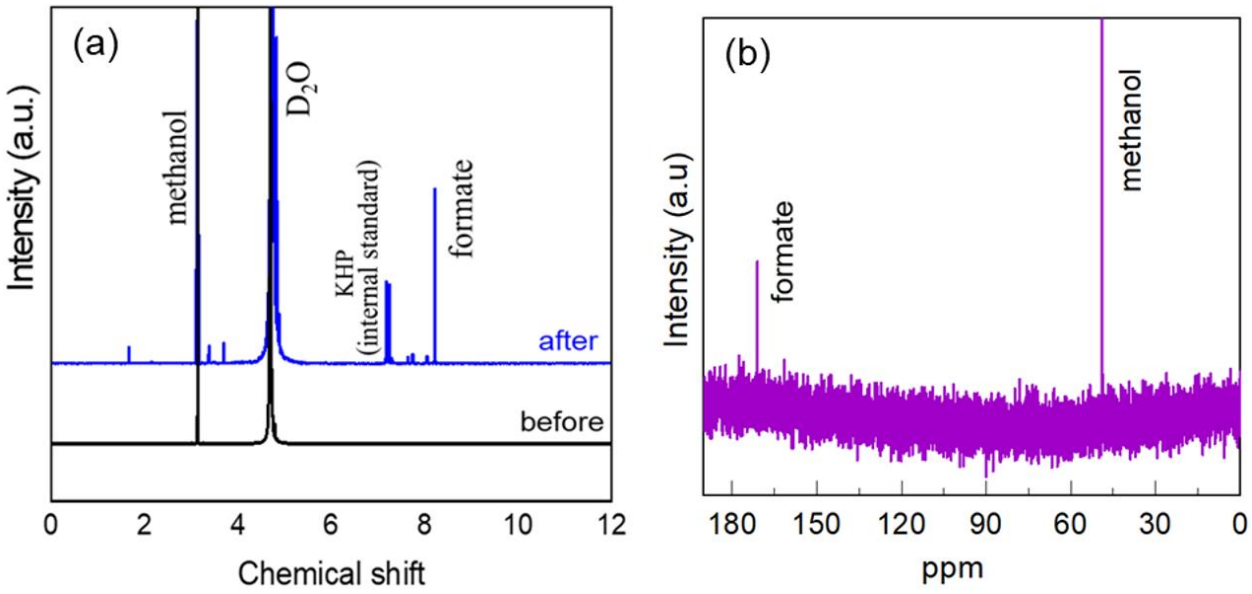


**Figure S12**. (a) $^{1}$H NMR spectra of 1.0 M methanol added 1.0 M KOH electrolyte after electrolysis for 5 hours at 50 mA.cm$^{-2}$. (b) $^{13}$C NMR spectra of 1.0 M methanol added 1.0 M KOH electrolyte after electrolysis for 5 hours at 200 mA.cm$^{-2}$.

Amount of electrolysis format was determined using $^{1}$H NMR analysis with KHP as the internal standard with the following equation.

$\frac{\mathbf{n}x}{\mathbf{n}y} = \frac{\mathbf{I}x}{\mathbf{I}y} \times \frac{\mathbf{N}y}{\mathbf{N}x}$ ..... (i), where $n_y$ and $n_x$ are the concentration of formate and KHP in the NMR samples, $I_x$ represents the integral area of the $^{1}$H NMR spectra for KHP, $N_x$ is the number of nuclei for KHP, $I_y$ represents the integral area of the product formed, and $N_y$ is the number of nuclei for the product. The amount of hydrogen gas evolved at the cathode was determined using the classical water displacement method.

The Faradaic efficiency (EF) was estimated using the following equation.

$FE(\%) = \frac{\mathbf{n}\times\mathbf{z}\times N_A\times\mathbf{e}}{\mathbf{Q}} \times 100$ ..... (ii), where n represents the number of moles of the electrolysis products, z (= 4 for format formation from MeOR) is the number of electrons

involved in the electrolysis, $N_A$ is Avogadro constant, ($6.02\times10^{23}$ $mol^{-1}$) constant, e is elementary charge ($1.60\times10^{-19}$ C) and Q (coulomb) is the total electricity consumed in the electrolysis process.

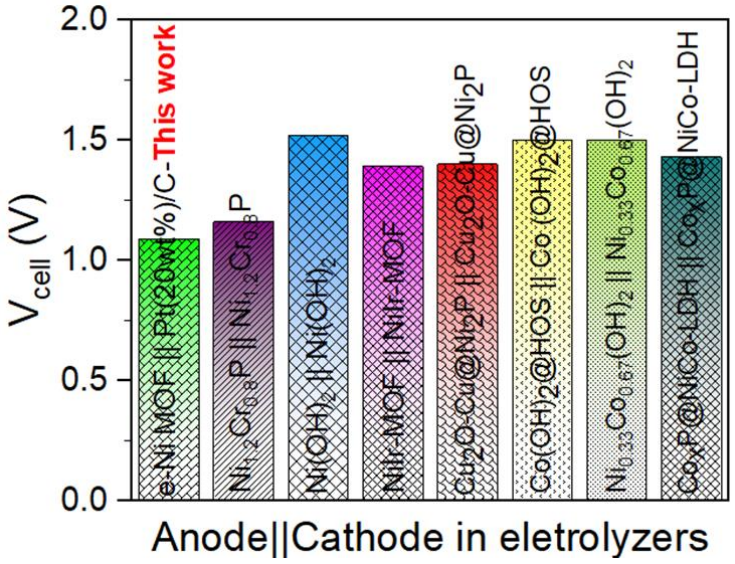


**Figure S13**. Cell voltages of various anode-cathode based electrolysers in alkaline water electrolysis at the benchmark current density of 10 $mA.cm^{-2}$.

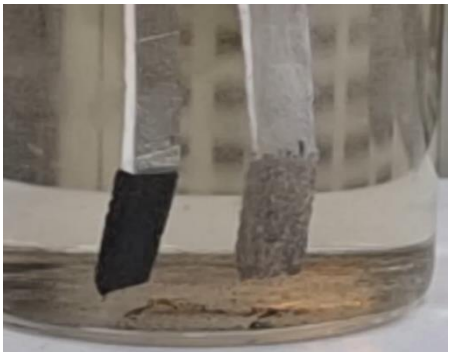

**Figure S14**. The dark electrode at left hand side is e-Ni MOF/NF (anode) and light one at right hand side is Pt (20wt%)/C/NF (cathode). To realize the hydrogen evolution at the cathode during MeOR at anode, see FigureS14-Video.mp4.

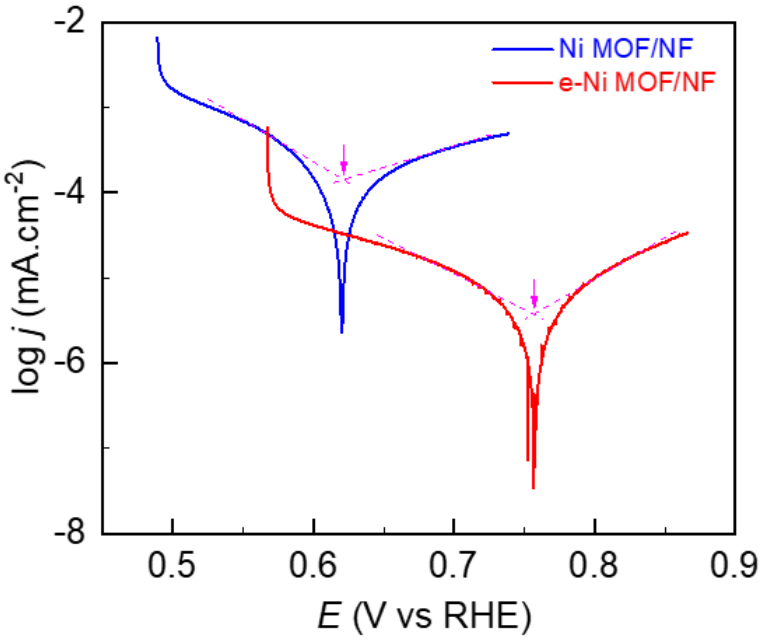


**Figure S15**. Tafel extrapolation curves of the pristine and e-modulated Ni MOF-based electrodes studied in 1.0 M methanol added 1.0 M KOH-based seawater electrolyte. Arrows indicate the point corresponding to the corrosion potential and corrosion current density.

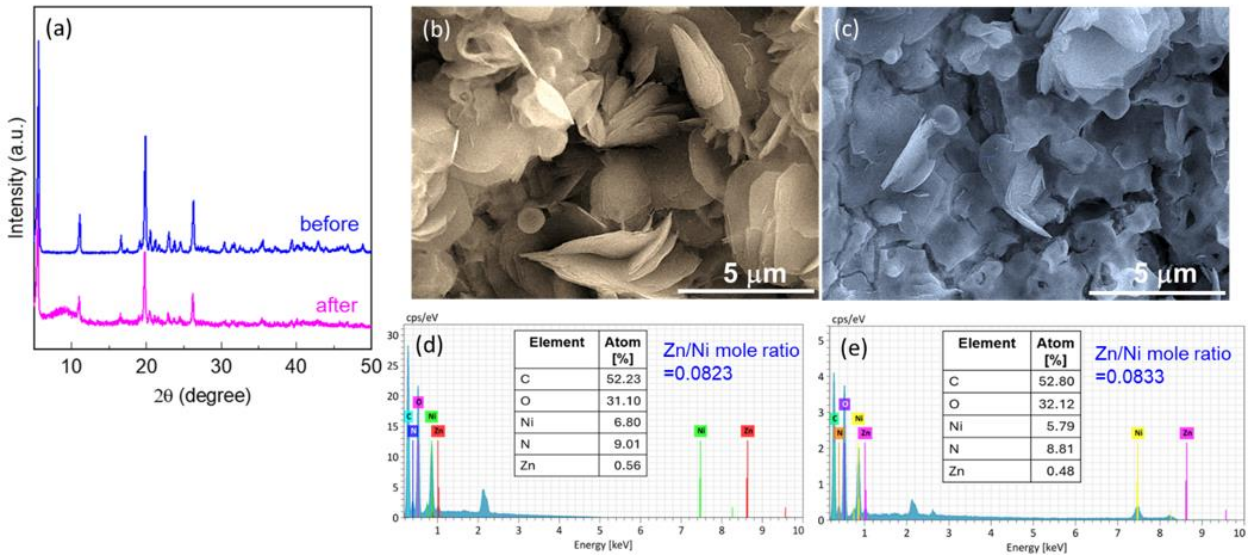


**Figure S16**. (a) PXRD of the e-Ni MOF before and after the long-term electrolysis over 48 hours at 10 mA.cm$^{-2}$ in 1.0 M methanol added 1.0 M KOH solution. SEM top surface views of the e-Ni MOF film (b) before, and (c) after the long-term electrolysis. Corresponding EDX spectra chemical composition of the e-Ni MOF before and after the long-term electrolysis.

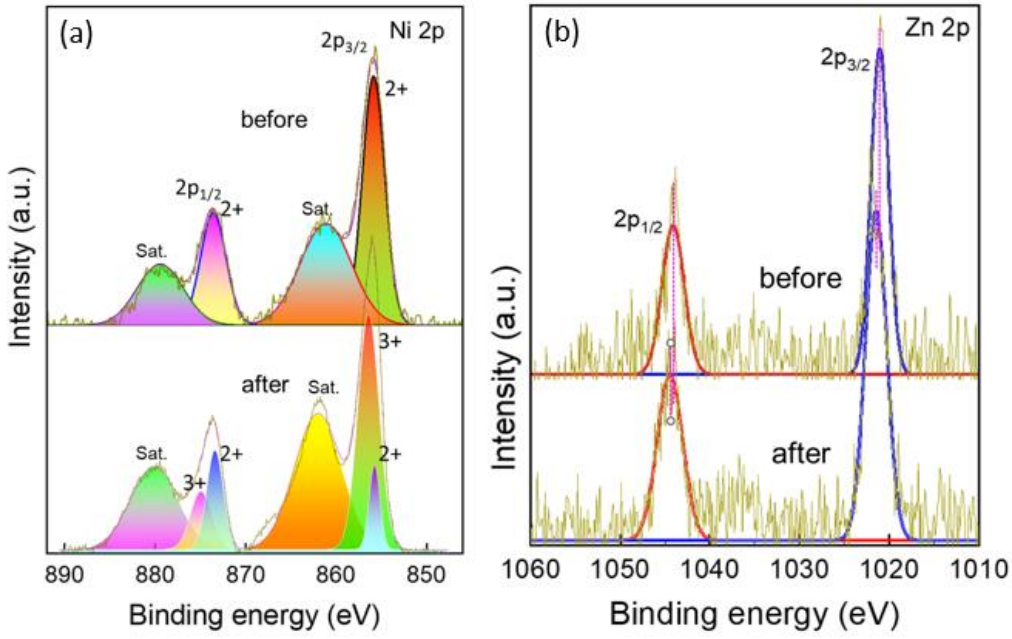


**Figure S17**. (a) Ni 2p and (b) Zn 2p, XPS spectra of the e-Ni MOF/NF electrode before and after the long-term electrolysis over 48 hours at 10 mA.cm$^{-2}$ in 1.0 M methanol added 1.0 M KOH solution.

**Table S1**. Performance comparison of high-performance MeOR electrocatalysts.

| **Catalyst** | **electrolyte** | **Scan rate** ($mVs^{-1}$) | ***E*** (V vs RHE) | **MeOR activity@** ***j*** ($mA.cm^{-2}$) | **Ref** |
|---|---|---|---|---|---|
| $Ni(OH)_{2–0.25}$ | 1 M KOH + 1 M $CH_3OH$ | 10 | 1.5 | 171.80 | [1] |
| $NiCo_2O_4$-450-Vo | 1 M KOH + 1 M $CH_3OH$ | 50 | 1.5 | ~ 50.00 | [2] |
| $Ni_{12}P_5$ | 1 M NaOH + 1 M $CH_3OH$ | 10 | 1.5 | ~ 70.00 | [3] |
| NiCo-MOF-P | 1 M NaOH+ 0.5 M $CH_3OH$ | 10 | 1.5 | ~ 115.00 | [4] |
| NiB-400 | 1 M KOH + 1 M $CH_3OH$ | 20 | | ~ 110.00 | [5] |
| NiSe/RGO-550 | 1 M KOH + 0.5 M $CH_3OH$ | 50 | 1.5 | ~ 28.00 | [6] |
| $Ni_{0.75}Fe_{0.25}Se_2$ | 1 M KOH + 1 M $CH_3OH$ | 50 | 1.5 | 53.50 | [7] |
| NiO NTs-400 | 1 M KOH + 0.5 M $CH_3OH$ | 50 | 1.5 | 24.30 | [8] |
| $Ni_1Co_2P_x$ | 1 M KOH + 1 M $CH_3OH$ | 5 | 1.5 | ~ 52.00 | [9] |
| NiS NPs/C | 1 M KOH + 1 M $CH_3OH$ | 50 | 1.5 | ~ 48.00 | [10] |
| $Ni_{1.2}Cr_{0.8}P$ | 1 M KOH + 3 M $CH_3OH$ | 5 | 1.5 | ~ 120.00 | [11] |
| CoCu-UMOFN | 1 M KOH + 3 M $CH_3OH$ | 5 | 1.5 | ~ 100.00 | [12] |
| $Ni(OH)_2$/NF nanosheet arrays | 1 M KOH + 0.5 M $CH_3OH$ | 5 | 1.38 | ~ 350.00 | [13] |
| e-Ni MOF | 1 M KOH + 1 M $CH_3OH$ | 5 | 1.40<br>1.50 | 338.49<br>968.81 | This work |

**Table S2**. Performance comparison of electrolyzers with MeOR || HER anodic and cathodic reactions.

| Electrolyzer | Electrolyte | $V_{cell}$ (V) @ $j$=10 mA.cm$^{-2}$ | Ref |
|---|---|---|---|
| $Ni_{1.2}Cr_{0.8}P$ \|\| $Ni_{1.2}Cr_{0.8}P$ | 1 M KOH + 3 M $CH_3OH$ | 1.16 | [11] |
| $Ni(OH)_2$/NF \|\| $Ni(OH)_2$/NF | 1 M KOH + 0.5 M $CH_3OH$ | 1.52 | [13] |
| NiIr-MOF/NF \|\| NiIr-MOF/NF | 1 M KOH +4 M $CH_3OH$ | 1.39 | [14] |
| $Cu_2O$-Cu@$Ni_2P$/NF \|\| $Cu_2O$-Cu@$Ni_2P$/NF | 1 M KOH +1 M $CH_3OH$ | 1.40 | [15] |
| $Co(OH)_2$@HOS/CP \|\| Co $(OH)_2$@HOS/CP | 1 M KOH + 3 M $CH_3OH$ | 1.50 | [16] |
| $Ni_{0.33}Co_{0.67}(OH)_2$/NF \|\| $Ni_{0.33}Co_{0.67}(OH)_2$/NF | 1 M KOH + 0.5 M $CH_3OH$ | 1.50 | [17] |
| $Co_xP$@NiCo-LDH/NF \|\| $Co_xP$@NiCo-LDH/NF | 1 M KOH + 0.5 M $CH_3OH$ | 1.43 | [18] |
| e-Ni MOF \|\| Pt(30wt%)/C | 1 M KOH + 1 M $CH_3OH$<br>30 wt% KOH +1M $CH_3OH$<br>30 wt% KOH +1 M $CH_3OH$ + Seawater | @$j_{10}$ = 1.33<br>@$j_{10}$ = 1.09<br>@$j_{10}$ = 1.10<br>@$j_{100}$ = 1.56<br>@$j_{400}$ = 1.75 | This work |

## S.I. References


1. L. Li, W. Gao, M. Lei, and D. Wen, *Chem. Eur. J.*, 2021, **27**, 10966–10972.
2. S. Chen, D. Huang, D. Liu, H. Sun, W. Yan, J. Wang, M. Dong, X. Tong and W. Fan, *Appl. Catal. B*, 2021, **291**, 120065.
3. S. Ghosh, B. Mondal, S. Roy, M. Shalom and M. B. Sadan, *J. Mater. Chem. A*, 2022, **10**, 8238–8244.
4. M. M. Rajpure, H. S. Jadhav, H. Kim, Colloids Surf. A: Physicochem. Eng. Asp., 2022, **654**, 130062.
5. Y. Qi, Y. Zhang, L. Yang, Y. Zhao, Y. Zhu, H. Jiang and C. Li, Nat. Commun., 2022, **13**, 4602.

6. J. Jia, L. Zhao, Y. Changa, M. Jiaa, Z. Wen, *Ceram. Int*., 2020, **46**,10023–10028.

7. J. Li, C. Xing, Y. Zhang, T. Zhang, M. C. Spadaro, Q. Wu, Y. Yi, S. He, J. Llorca, J. Arbiol, A. Cabot, and C. Cui, *Small*, 2021, **17**, 2006623.

8. T.-J. Wang, H. Huang, X.-R. Wu, H.-C.Yao, F.-M.Li, P. Chen, P.-J. Jin, Z.-W. Deng and Y. Chen, Nanoscale, 2019, **11**, 19783–19790.

9. S. Chen, X. Yang, X. Tong, F. Zhang, H. Zou, Y. Qiao, M. Dong, J. Wang, and W. Fan, *ACS Appl. Mater. Interfaces*, 2020, **12**, 34971−34979.

10. J. Li, X. Tian, X. Wang, T. Zhang, M. C. Spadaro, J. Arbiol, L. Li, Y. Zuo, and A. Cabot, *Inorg. Chem*. 2022, **61**, 13433−13441.

11. U. P. Suryawanshi, U. V. Ghorpade, J. A. Yuwono, P. V. Kumar, M. A. Gaikwad, S. W. Shin, J. S. Jang, H. R. Jung, M. P. Suryawanshi and J. H. Kim, *J. Mater. Chem. A*, 2024, **12**, 15127–15136.

12. X. Wei, S. Wang, Z. Hua, L. Chen, and J. Shi, *ACS Appl. Mater. Interfaces*, 2018, **10**, 25422−25428.

13. J. Hao, J. Liu, D. Wu, M. Chen, Y. Liang, Q. Wang, L. Wang, X. Z. Fu and J. L. Luo, *Appl. Catal. B*, 2021, **281**, 119510.

14. Y. Xu, M. Liu, M. Wang, T. Ren, K. Ren, Z. Wang, X. Li, L. Wang and H. Wang, *Appl. Catal. B*, 2022, **300**, 120753.

15. L. Li, L. Zhang, L. Gou, S. Wei, X. Houa and Li W., *Chem. Eng. J*. 2023, **454**, 140292.

16. K. Xiang, D. Wu, X. Deng, M. Li, S. Chen, P. Hao, X. Guo, J. L. Luo and X. Z. Fu, *Adv. Funct. Mater*., 2020, **30**, 1909610.

17. M. Li, X. Deng, K. Xiang, Y. Liang, B. Zhao, J. Hao, J.-L. Luo and X.-Z. Fu, *ChemSusChem,* 2020, **13**, 914 – 921.

18. M. Li, X. Deng, Y. Liang, K. Xiang, D. Wu, B. Zhao, H. Yang, J.-L. Luo, X.-Z. Fu, *J. Energy Chem*., 2020, 50, 314–323.